JUICE Attitude and Orbit Control System : major HW & SW challenges from design to development & validation

P. Regnier [1], J. Grzymisch [2]

[1] Airbus Defence and Space (SAS), rue des Cosmonautes 31400 Toulouse (France)
[2] European Space Agency
pascal.regnier@airbus.com, jonathan.grzymisch@esa.int

ABSTRACT

The JUICE - JUpiter ICy moons Explorer – mission is the first large-class mission in ESA's Cosmic Vision 2015-2025 programme. Launched on April 14th 2023 by the last-but-one Ariane 5, it will arrive at Jupiter in July 2031 and then spend at least three years making detailed observations of the giant gaseous planet and three of its largest moons, Ganymede, Callisto and Europa, through more than 35 fly-bys and a final orbiting phase around Ganymede, becoming the first spacecraft to orbit a moon of another planet. Airbus Defence and Space Toulouse was selected as Prime Contractor in July 2015, and is also responsible for the design and development of the AOCS Subsystem and the on-board Software. This paper focuses on the JUICE AOCS HW development and validation achievements and the first in-orbit results (SW validation of complex functions mandatory at Jupiter like Fail-Operational manoeuvre modes and autonomous navigation is under completion on-ground during the early cruise phase and will be subject of another publication). Since the previous JUICE AOCS paper presented six years ago at the ESA GNC Conference in Graz, AOCS equipment suppliers and Airbus, together with ESA, have made all efforts to progress on the development and qualification of AOCS HW that best meet the demanding JUICE mission objectives and requirements. All these efforts now materialize through a priceless reward being a – for the moment – flawless in-flight AOCS behaviour and excellent performance.

1 INTRODUCTION : JUICE basics

1.1 JUICE Mission Scenario

After its picture-perfect VA260 launch by Ariane 5 on April 14th 2023, JUICE will cruise during 8.5 years, with three Gravity Assists at Earth (one with Lunar Gravity Assist) and one at Venus. The early phase of the cruise trajectory in the inner Solar System imposes stringent constraints at thermal level, forcing to maintain a fixed Sun-pointed attitude even in case of failure, and a low Sun incidence on the solar arrays to limit their temperature. The spacecraft is then captured around Jupiter on a highly elliptical orbit thanks to a critical insertion manoeuvre of about 800m/s preceded by a Ganymede fly-by 7.5h before, aimed at reducing the ΔV amplitude. After 6 months spent on the first orbit with a perijove raising manoeuvre at its apojove, several Ganymede fly-bys are used to reduce the orbit energy and then initiate a Europa science phase consisting in two low altitude fly-bys, before entering into a Jupiter high latitudes phase (up to 33°) through multiple Callisto fly-bys. After about 2 years orbiting Jupiter the spacecraft is then transferred to Ganymede through another fly-bys sequence which ends with a gravitational capture manoeuvre into an eccentric orbit around Ganymede with a 10000km apocentre. Science will be performed on this eccentric orbit during 150 days then followed by a circularisation manoeuvre to support a 130-day science phase from a 500 km altitude orbit, before naturally crashing on the moon due to the effect of Jupiter on orbit stability. The total ΔV budget is about 2.2 km/s and the overall mission duration up to 13 years. The quasi-optimal launch date reached inside the launch window and the perfect injection of JUICE on its Earth escape orbit by Ariane 5 might even allow to lower the Ganymede Science circular orbit to an altitude of 200km at End-Of-Life before the planned crash on the surface.
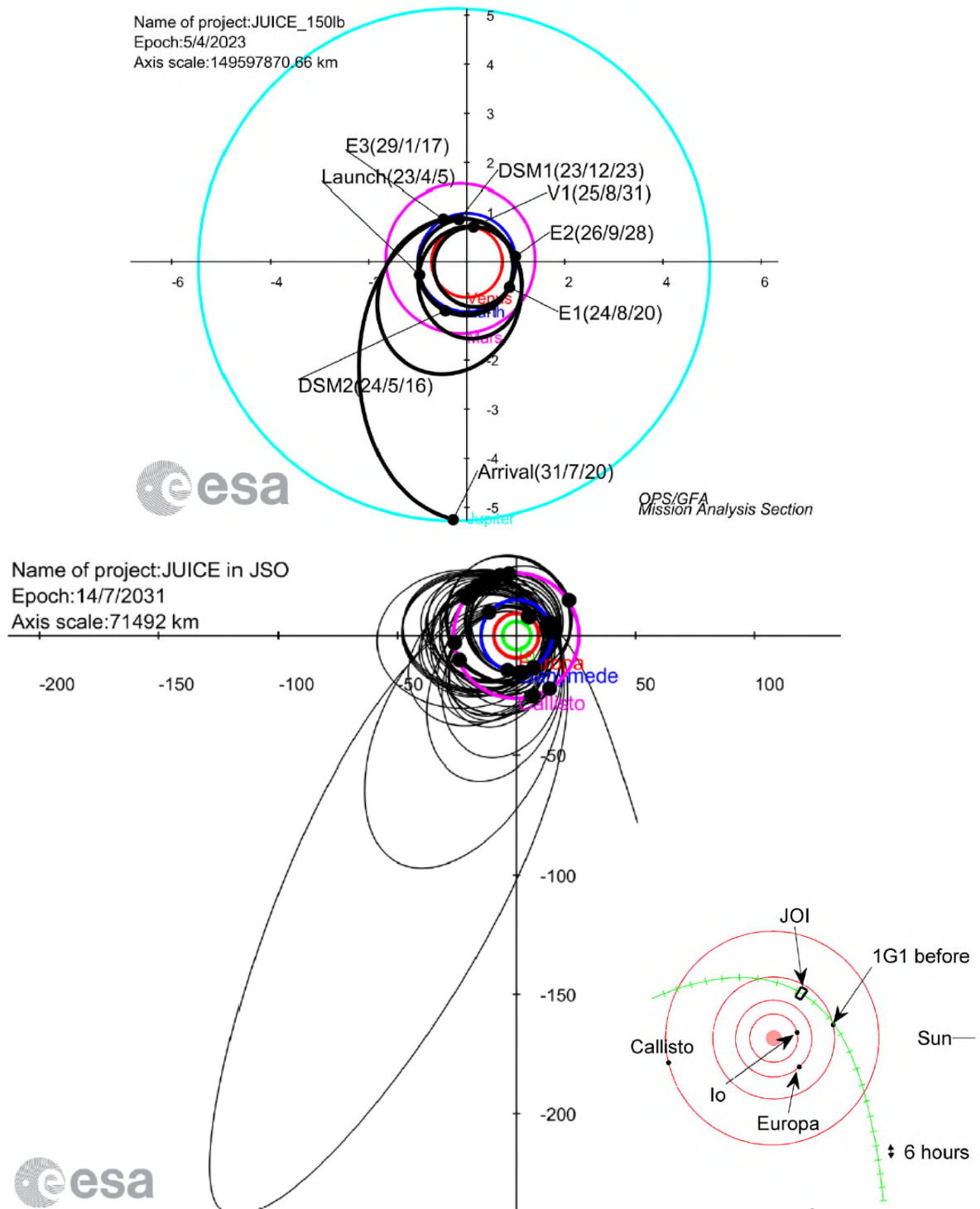
Figure 1. JUICE baseline cruise and Jupiter tour trajectories

A major constraint at mission level is the total radiation dose cumulated at End-Of-Life and the worst case peak electrons flux received during the two Europa fly-bys, both due to the harsh radiative environment around Jupiter, as illustrated on Figure 2. These were strong design drivers for the AOCS equipment development and qualification, preventing the re-use of recurrent HW without modifications, even those qualified for GEO applications. The total radiation dose during the mission is 256 krad under 10 mm aluminium spheres shielding, 10% of which is brought by the Europa phase and 40% by the Ganymede orbiting phase.
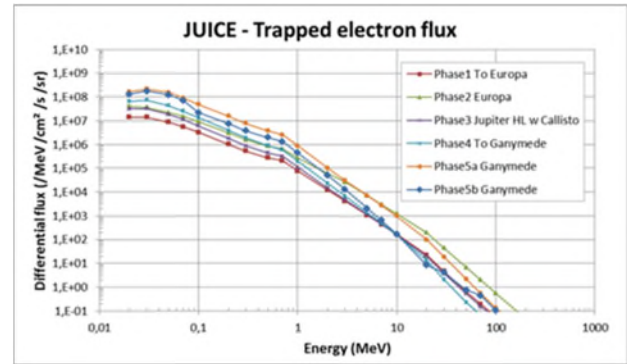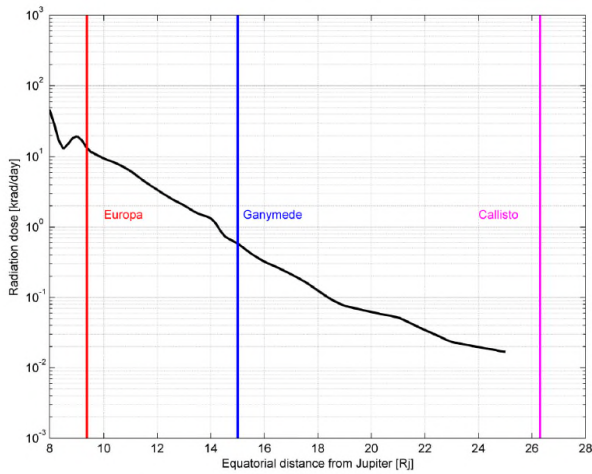
Figure 2. Daily Radiation dose as a function of distance to Jupiter and worst case electron flux

1.2 JUICE Spacecraft Configuration

The JUICE spacecraft configuration is shown on Figure 3. The central body of 4x2x2m size is built around a central tube accommodating two large propellant tanks of 1600 litres each, with the main engine of 450N installed centrally at the bottom of the tube. In addition to the two huge cross-shaped solar arrays wings of 45m2 area each, the other deployed appendages are a 10.5m long magnetometer boom at the lower end of the central body, a 16m-long radar antenna at the top, and four 2m-long arms supporting Langmuir probes. The nadir-pointed face is along +Z axis, a 2.4m diameter fixed High Gain Antenna is accommodated on the –X face, and most scientific instruments are mounted on an optical bench on the +X face, together with the Star Tracker Optical Heads. A 0.5m diameter 2-axis articulated Medium Gain Antenna completes the communication subsystem suite. This JUICE spacecraft configuration raises unique challenges on AOCS due to flexibilities of multiple and large appendages with a widespread and uncertain frequency range, large propellant tanks with massive propellant sloshing modes, and a main engine to be fired with large deployed solar arrays, which is very uncommon in space missions.

The spacecraft features two vaults aimed at protecting sensitive electronic boards of platform and scientific instruments from the harsh jovian radiation environment. They accommodate a layer of 1mm thick lead weighting about 100 kg.

Figure 3. JUICE Spacecraft configuration

1.3 JUICE AOCS HW Baseline

The JUICE AOCS architecture is classical of an interplanetary mission, based on gyro-stellar attitude measurements and reaction wheels for attitude control. It relies on two analogic internally-redunded Sun sensors, one triple-head Star Tracker with redunded electronics, two Inertial Measurement Units (3-axis gyros and accelerometers), four high capacity reaction wheels, and one redunded navigation camera. All equipments are connected to the Command and Data Management Subsystem either via a 1553 bus or through the Remote Interface Unit except the navigation camera connected directly to the On-Board Computer via Spacewire links.
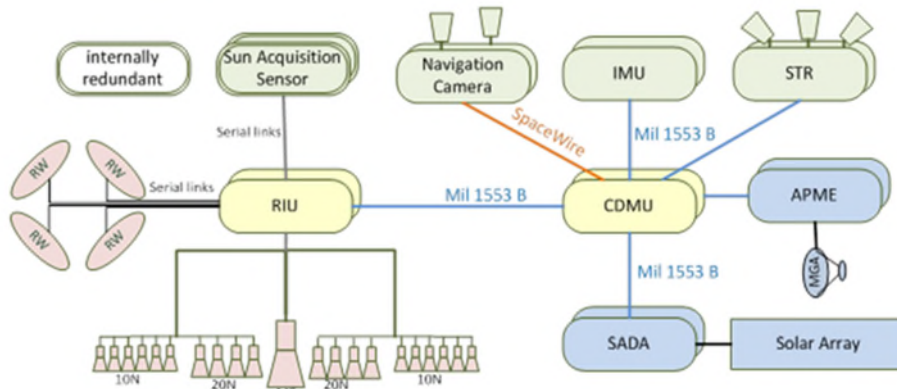

Figure 4. JUICE AOCS HW Architecture

The thruster configuration features four redunded 22N thrusters at the bottom of the spacecraft and aligned with the Main Engine thrust to support attitude control during the ME boost and also to implement smaller axial trajectory manoeuvres without the ME, at moderate thrust. A small tilt angle transverse to the Spacecraft longitudinal axis allows these thrusters to achieve 3-axis attitude control. Six additional redunded 10N thrusters complete the thruster configuration to support pure torque 3-axis attitude control and transverse thrust capability especially useful for the attitude-constrained inner cruise phase.

2 JUICE AOCS Equipment Development Challenges

2.1 JUICE High-Performance Autonomous and Robust Star Tracker

The JUICE Star Tracker is provided by SODERN and is highly inherited from the HYDRA generic product, it features two separate Electronic Units installed inside the Spacecraft vaults and cross-strapped to three Optical Heads co-located near the scientific instruments on the Optical Bench. Despite numerous spacecraft accommodation constraints of Field-Of-View clearance from multiple deployed appendages and a spacecraft Ganymede nadir-pointing attitude on the low altitude Science orbit with no star obstruction by the huge Ganymede apparent diameter, it was possible to implement large inter-head angles between 45° and 55° such that continuous multi-head fusion can maximise attitude estimation performance and robustness.

In addition, SODERN, Airbus and ESA carefully assessed the required evolutions from the generic HYDRA product in order to make it more robust to the harsh jovian environment while keeping it still affordable and with a reasonable mass increase (see reference 1). Finally the following HW and SW upgrades have been implemented to best achieve these difficult challenges :
* Spot / local shielding in Electronic Unit
* Shielding shell around OH bottom part

- SW upgrades :
    - Parameters re-tuning (integration time, background thresholds…)
    - Rate assistance availability on-the-fly, not only at initialisation
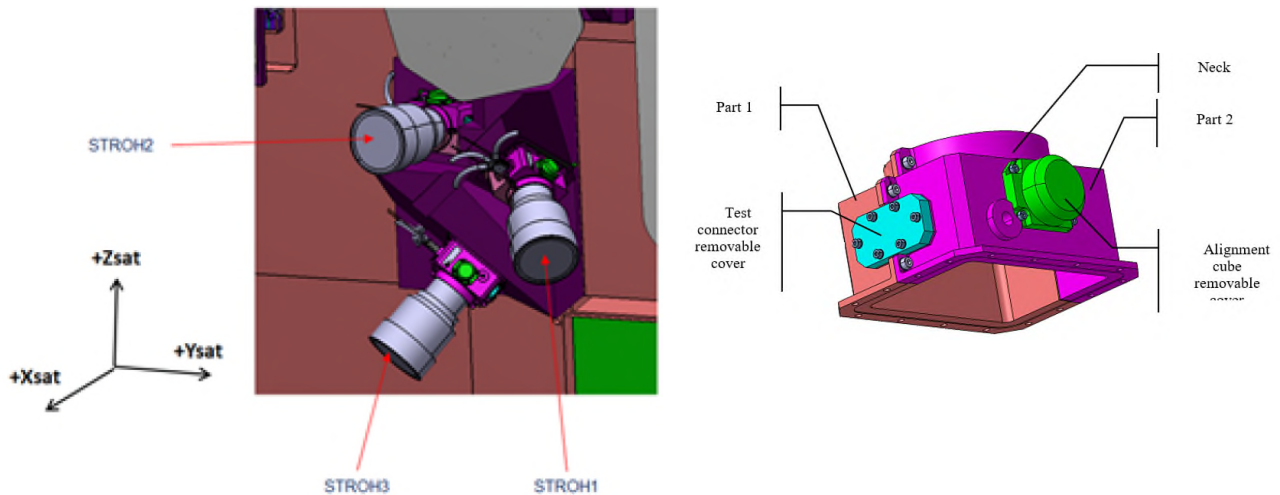   - Mode-specific improvements (designated acquisition with largest possible star window size…)

Figure 5. JUICE HYDRA Star Tracker Configuration and specific OH shielding

SODERN has carefully assessed the JUICE HYDRA Star Tracker intrinsic performance and robustness of the tracking and Lost-In-Space Acquisition modes through high fidelity numerical simulations involving raw-level effects of radiation protons and electrons on the APS detector (ATOS simulation tool). The demonstrated tracking mode robustness remains excellent even during Europa fly-bys, being the harshest radiation environment during the mission (and one of the most important science-wise). As shown in Figure 6, tracking mode maintenance is ensured at 100% probability when at least two OHs are available, and when rate-assistance is provided to the sensor from AOCS SW, which is the baseline during these critical short periods, the tracking mode robustness is ensured event with only one OH. Under harsh radiation conditions, the Lost-In-Space acquisition mode experiences longer than nominal acquisition durations but thanks to appropriate dynamic conditions and rate assistance ensured by the AOCS SW during the Sun-pointed Survival Mode there should be no dead-end situation, the transition to tracking being successful after at most 30 minutes. Even in the very improbable case where the STR would fail to acquire, the ultimate survival mode consisting in a spinning Earth Strobing attitude stopped by ground operators in a 3-axis stabilized Sun/Earth pointed attitude after detecting the maximum amplitude of an RF signal emitted by the Medium Gain Antenna, would support a tracking mode recovery operation using the STR Designated Acquisition mode with a ground-uplinked quaternion, which is always successful after 50s.

The tailoring of some STR SW parameters to the specific JUICE mission radiative environment has naturally decreased the robustness of the HYDRA star tracker to dynamic conditions, which is normally one of its major outstanding features, but this is not at all detrimental to the JUICE mission attitude measurement availability, due to the combination of reasonable kinematic conditions in all AOCS modes requesting an attitude measurement from the STR, huge spacecraft inertia and the presence of gyros.

Furthermore the improvement of the JUICE HYDRA star tracker robustness to radiations did not degrade the achievable attitude measurement accuracy at all, which remains comfortably within the required attitude estimation performance specification in Science mode (5arcsec half-cone at 2σ).
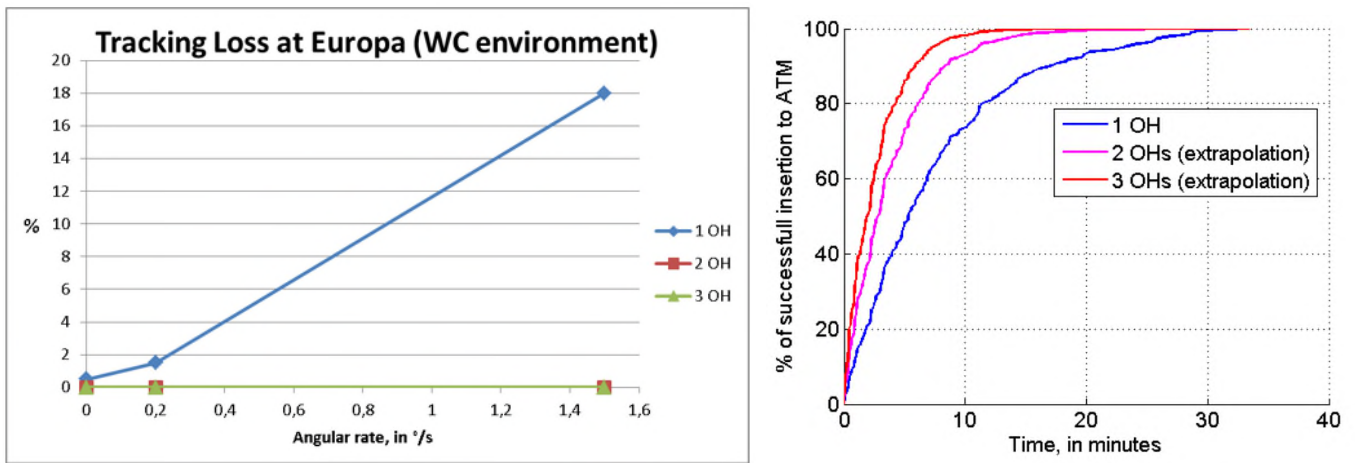
Figure 6. JUICE HYDRA Star Tracker Tracking mode and Lost-in-Space Acquisition mode robustness statistics

This intrinsically improved star sensing robustness is also combined with AOCS SW tailored functional commanding of the STR aimed at maximising the probability of maintaining the star tracking mode and recovering it in case of tracking loss :

-   Continuous operation with 3 OHs in hot redundancy to maximise tracking and acquisition robustness and attitude measurement performance
-   Commanding in aided tracking with the estimated attitude from the gyro-stellar estimator in case of loss of tracking without STR autonomous re-acquisition success through Lost-In-Space acquisition within a short duration (minutes), while the GSE attitude is accurate within less than 0.1°
-   Commanding in Designated Acquisition with the GSE attitude afterwards, with adequate parameterization and during typically one hour, being compatible with attitude errors up to 1.5°
-   Then the STR is reset and commanded back to Lost-In-Space Acquisition, in order to cut the link between AOCS SW and STR, which could be detrimental in case of non-nominal conditions
-   Rate assistance near Europa environment and ground-commanded change of STR Lost-In-Space acquisition SW parameters to improve robustness
-   Ground-uplinked Designated Acquisition in Earth Strobing survival mode

2.2   JUICE Navigation Camera

The JUICE Navigation Camera will serve two main purposes during the mission :

1. Provide optical navigation inputs to the ESOC Flight Dynamics team during the Jupiter Tour, in order to complement ground-based radiometric measurements and improve the current ephemerides knowledge of jovian moons, and the Spacecraft relative position to the moons especially priori to low altitude fly-bys

2. Support the on-board autonomous navigation SW named EAGLE for "Enhanced Autonomous Guidance through Limb Extraction", which consists in acquiring jovian moons close-range NavCam images during fly-bys to be processed by an on-board Image Processing Software able to compute the Spacecraft 3-axis relative position by identifying the moons limb. This position measurement is then fed into an extended Kalman filter which continuously propagates the S/C relative position and velocity vectors, which are used to update the nadir-pointing reference necessary to achieve the Science pointing profile with the specified accuracy. Indeed due to the navigation cut-off latency of 2 days prior to each fly-by, ground navigation alone cannot meet the Science pointing performance need through ground–

uplinked profiles, and ESOC will rely on EAGLE to update those profiles autonomously on-board (as well as the Time of Closest Approach) during early jovian moon fly-bys, as long as ephemerides are not accurate enough.

The JUICE NavCam is provided by SODERN and is based on their high heritage in star trackers and space optical instruments. It is a monoblock camera comprising a Detector Unit implementing a 1024x1024 pixels HAS2 Active Pixel Sensor detector known for its high robustness to harsh radiation environments and a thermo-electrical cooler, a Lens Assembly with Rad Hard glasses encompassing a 4° Field-Of-View, and a Baffle assembly providing a Sun Exclusion Angle of 30°. The electronic Unit, being accommodated outside the S/C vaults, is carefully shielded and includes a Rad Hard 16Mb MRAM (instead of EEPROM) and a Rad Hard FPGA in order to optimize its robustness to radiations.

The NavCam FPGA encompasses two main modes, a Raw Imaging mode aimed at acquiring extended objects at low integration times and high image quality (PSF, ESF, optics aberration and thermal stability), and a Star Centroiding mode where up to 12 detection windows are opened either directly by TC or by the AOCS SW using a ground-uplinked star catalog of reduced size for each relevant mission phase, allowing detection and fine measurement of stars up to magnitude 8.8, with an integration time up to 5s. Stars measurements are mandatory in order to reference the measured Line Of Sight to jovian moon centers in an inertial frame, they are also used to calibrate the NavCam alignment with respect to the gyro-stellar reference;

The major technical challenges successfully addressed by SODERN included the in-field straylight (stars must be acquired and measured with a bright jovian moon in the middle of the FOV), the star centroiding robustness and performance despite the harsh radiative environment (an electrons filtering algorithm is used to mitigate the impact of electrons fluxes and avoiding saturation due to straylight), and the accurate simulation and performance prediction of the Star Centroiding and Imaging Modes. For the latter SODERN used their in-house ATOS simulation tool which accurately simulates all effects including optical performances and motion blur (transmission, PSF and straylight), HAS2 electro-optical performances (photo response, cross-talk, full well capacity, readout noise, dark current, FPN, PRNU, photonic noise, ADC quantification and saturation), HAS2 readout modes (rolling shutter, full frame and windowed sequencing), Radiation induced cumulative effects (optical transmission loss, HAS2 dark current, DSNU, spikes), Radiation induced transient effects (Cherenkov and luminescence photons, Jovian electrons induced ionization effects of HAS2 3D pixel array). This allowed to efficiently predict single-star and attitude determination performances, as well as providing to the Airbus Image Processing team detailed NavCam numerical models then used in combination with the Surrender virtual scene rendering SW to consolidate the EAGLE performance.
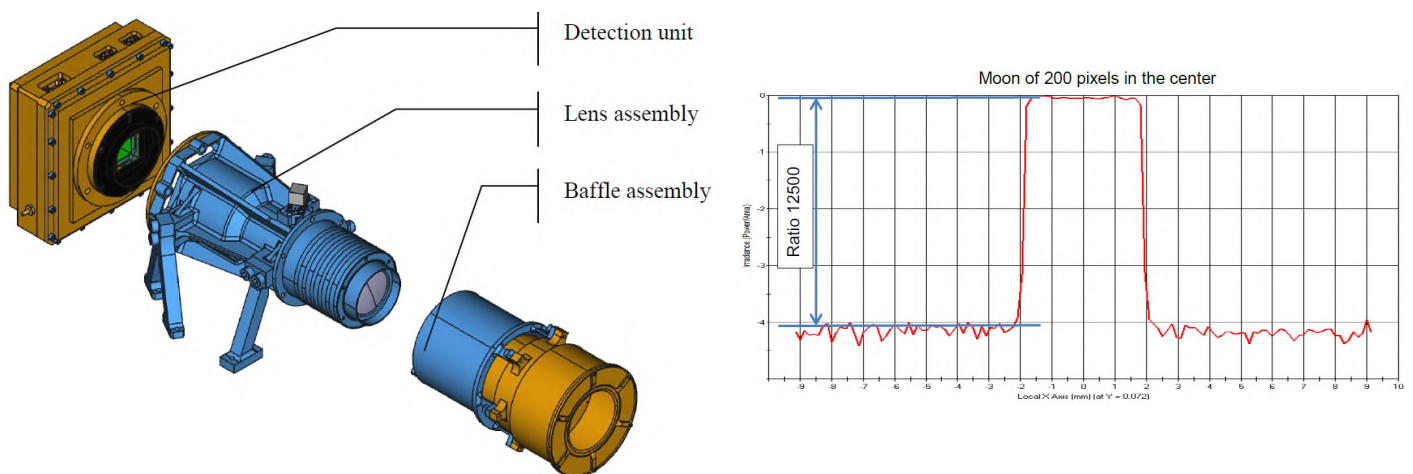

Figure 7. JUICE Navigation Camera Configuration and in-field straylight performance
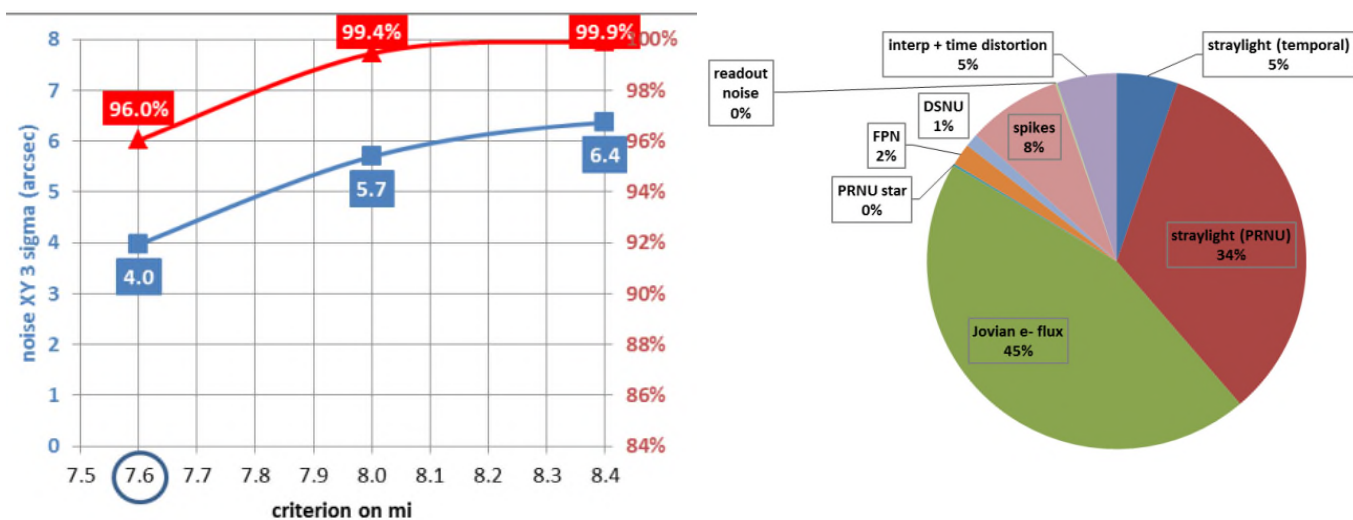
Figure 8. JUICE Navigation Camera NEA and vault coverage statistics

2.3 JUICE Inertial Measurement Unit

The JUICE Inertial Measurement Unit is a modified Miniature Inertial Measurement Unit (3.2 version) from Honeywell (USA) encompassing three Ring-Laser gyrometers and three QA3000 accelerometers. Two cold-redundant IMUs with co-linear measurement axes are co-located in the S/C +X Vault. This IMU is already Rad-Hard by design but its robustness to radiations has been re-enforced through a re-design of the mechanical chassis and top cover with enlarged thickness, including also the addition of Tantalum plates inside and at the bottom, for an extra mass of 3.6kg compared to the standard MIMU product.

The MIMU from Honeywell being ITAR-controlled no further details can be published in this paper.
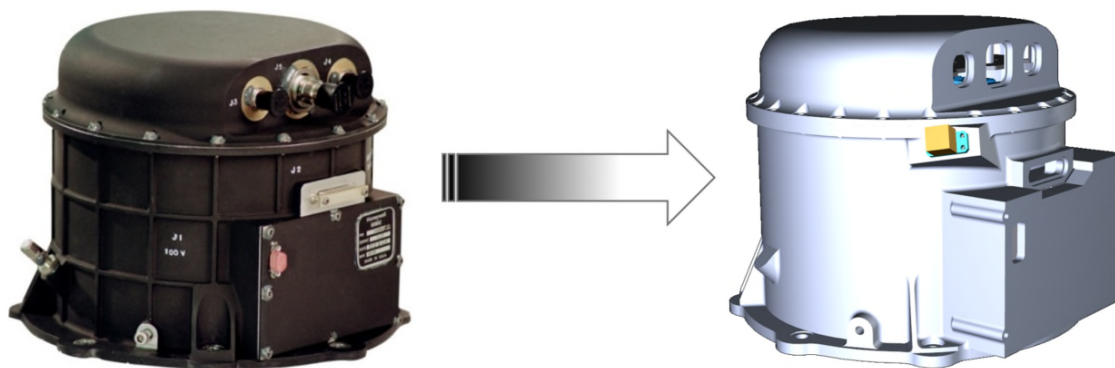

Figure 9. JUICE Inertial Measurement Unit

2.4 JUICE Reaction Wheels

JUICE relies on four powerful reaction wheels to achieve a smooth and high accuracy attitude control. The four wheels are placed in a pyramidal configuration within Spacecraft cavities around the central cylinder, as they could not be located inside the vaults due to limited volume constraints.

The JUICE Reaction Wheel is a new development from Collins Aerospace (ex RCD), the RSI 68-220/60, meaning that it provides an angular momentum of 68Nms at a rotational speed of 6000rpm, and a maximum control torque of 220mNm. The design of the wheel is heavily based on RCD heritage, especially from Solar Orbiter for the mechanical parts and Alphabus for the electronics. It uses the space-proven DRALLRAD ball-bearing unit and integrated wheel drive electronics. The

electrical interface relies on a 100V input voltage with a reverse current re-injection on the system bus during braking, and the overall mass of each reaction wheel is about 12kg, mainly due to additional shielding and flywheel mass necessary to meet the 68Nms target.

Major design evolutions were mandatory in order to upgrade the electronics to increase the maximum rotational speed from 4500 to 6000rpm, and to meet the very stringent EMC requirements of the JUICE mission (especially magnetic cleanliness) and its harsh radiative environment, including :
- Additional shields made of Mu-metal inside the wheel in order to reduce its magnetic signature
- Motor magnets pre-selected with respect to their field strength in order to produce a more homogenous multipole field of the rotor assembly
- Establishment of a magnetic cleanliness control plan and demagnetization procedure during final assembly
- Specific design of the flywheel mass in a single piece of nonmagnetic Aluminium alloy, providing a reduced magnetic signature and extra radiation shielding
- Additional spot shielding plates within the embedded electronics
- Torque command interface through a PWM signal derived from the Alphabus Reaction Wheel, which is much more EMC-friendly than an analog current interface

These evolutions imposed to modify the PCB electronic layout and components soldering and go through a complete qualification program with technical issues and programmatic delays. Another difficulty was that the reaction wheels are mounted on dynamic isolators to minimise their microvibration impacts on the Payload pointing performance, resulting in a radiative instead of conductive thermal coupling, which exacerbated the thermal hot cases in high speed and acceleration conditions.

All these efforts produced by Collins Aerospace allowed to deliver powerful reaction wheels with an extraordinary magnetic cleanliness performance with an AC magnetic dipole moment below 1mAm² instead of 200mAm^2 for this class of product.
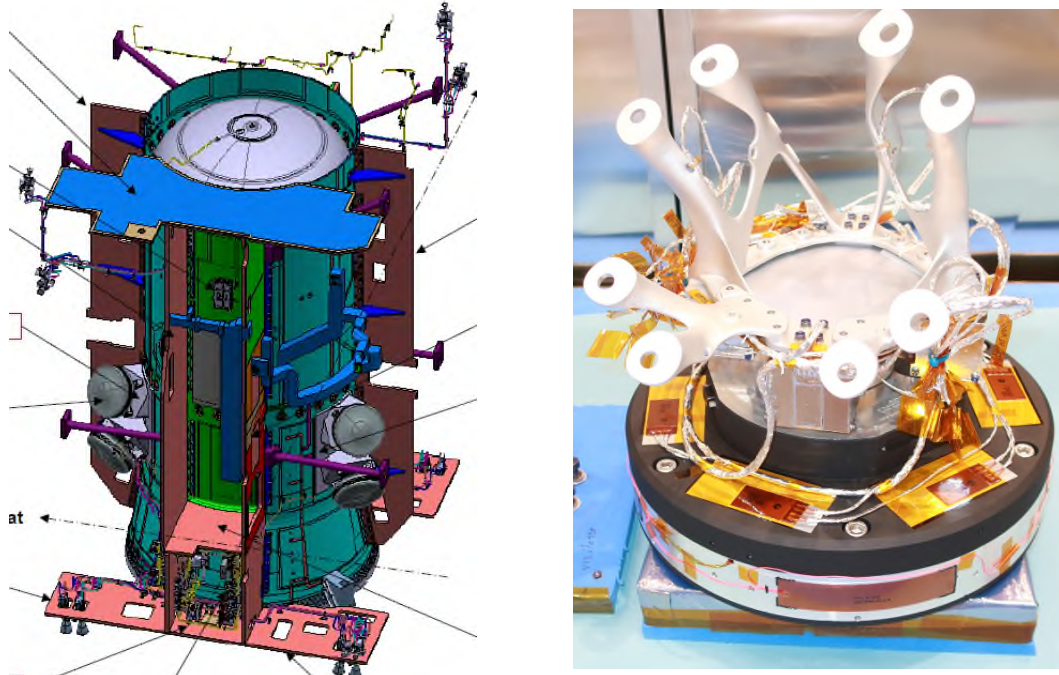

Figure 10. JUICE Reaction Wheels Configuration on S/C Structure and photo of a flight model with 3D-printed bracket and dynamic isolator

3   LEOP

The JUICE Launch and LEOP successfully took place on 14-15th of April 2023. Below is a timeline of the AOCS relevant events:

- Launch @ 12:14
- Separation date @ 12:42
- Telemetry acquisition @ 13:04
- First Sun Acquisition Mode (SAM) entry @ 13:01
- SAM Sun Biased Phase convergence @ 13:08
- Switch to Stand-by Mode (SBM) for Solar array (SA) deployment @13:27
- Solar Array (SA) deployment micro-switch confirmation @ 13:30 for Y+ and 13:33 for Y-
- Second SAM entry after SA deployment @ 13:42
- Solar Array Drive Electronics (SADE) ON @ 13:43
- Star Tracker (STR) ON @ 13:43
- SAM SBP converged @ 13:45
- SBM entry @ 17:10
- SAM RRP @ 17:00
- Safe Hold Mode (SHM) Slew Manoeuvre Phase (SMP) entry @ 17:01
- SHM Thruster Control Phase (TCP) entry @ 17:03
- RWs spin-up from 17:42 to 17:57
- SHM Coarse Pointing Phase (CPP) @ 19:56 (first wheel based mode)
- Set STR Julian date @ 20:45
- Transition to Normal Mode (NM) CPP @ 20:51
- Medium Gain Antenna (MGA) deployed successfully @ 3.30h
- End of LEOP

The Near Earth Commissioning Phase (NECP) begun immediately after the LEOP. This phase, which is still underway saw several AOCS related activities such as SAS bias calibration, STR OH bias calibration, and flexible mode characterization. This last activity is notable due to the many flexible modes JUICE has due to the various flexible appendages. The following paragraphs describe some of these phases and activities in more detail.

3.1   First SAM

After a few tense (nominal) minutes of wating for first contact, telemetry from the spacecraft was received after SAM convergence. Separation attitude around the spacecraft Z axis was expected to be random. As the two communication Low Gain Antenna (LGA) located on either side of the spacecraft perpendicular to the Z axis employ two different polarizations, it was expected that communications might not be established until after SAM convergence, as the ground had chosen to listen for a telemetry carrier with a fixed polarization. This was unfortunately the case, where the LGA with the correct polarization was pointing away from the earth, which combined with low separation rates resulted in some tense minutes before telemetry was established.

On telemetry reception, the CPS priming had been completed successfully, the SAM "Rate Reduction Phase" (RRP) had converged and the "Sun Capture Phase" (SCP) was underway, which was completed quickly afterwards. The separation rates and sun angles could be retrieved after dumping of the telemetry stores, and were observed to be in the order of 0.2deg/s mostly transverse to the separation axis Z, with the Sun passing prior to separation through the Field of View (FoV) of the Sun Acquisition Sensor (SAS) placed on the -X axis. The figure below shows the body rates and angles after separation. Note that the SAS being passive are acquired before separation, but the IMU was only activated by the automatic separation sequence after separation.
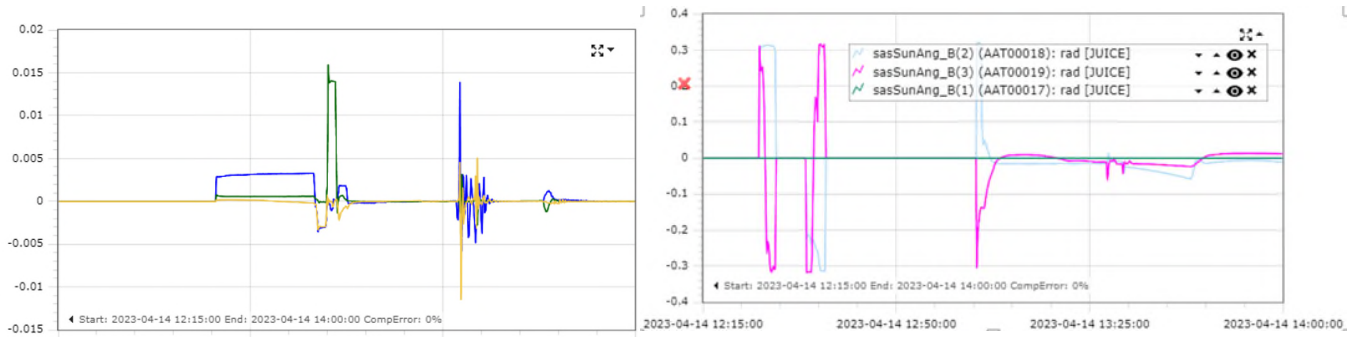
Figure 11. Body rates (top) and SAS angles (bottom) during separation.

3.2 Solar Array Deployment

The solar arrays were deployed autonomously without any observed anomaly, and SAM mode was re-activated autonomously afterwards, quickly recovering the ~5deg de-pointing acquired during deployment. Once the SADE was switched on, the SA angles, which were free to rotate during deployment, were measured at -98deg for Ym, 84.4deg for Yp, which was close to the expected positions.

3.3 Sensor Heath and Consistency Checks

On the Project Support side, an array of sensor checks were carried out to detect any anomaly, including consistency between prime and redundant branches where possible, as well as dissimilar sensors such as IMU-STR rates, IMU rates to expected rates from thruster actuations and expected sun position from orbit and STR quaternion vs Sun sensor readings.

Sun Acquisition Sensors (SAS)

During the spacecraft automatic initialization sequence, both prime and redundant Remote Interface Units (RIUs) were ON in order to fire propulsion system and solar array deployment pyros. This provided an opportunity to acquire the SAS currents from the redundant cells connected to the redundant RIU. Processing of these currents for calibration and sun angle computation allowed comparing both prime and redundant Sun angle readings and compare them to the on-board processed result. The following figure shows the sun angles as computed from the raw currents along with their difference, which presents a ~0.3deg bias between the prime and redundant cells. This was deemed acceptable as the SAS alignment specification is 0.5deg. Note that the angSAS_B telemetry is acquired at a higher rate than the currents, therefore resulting in the observed differences.
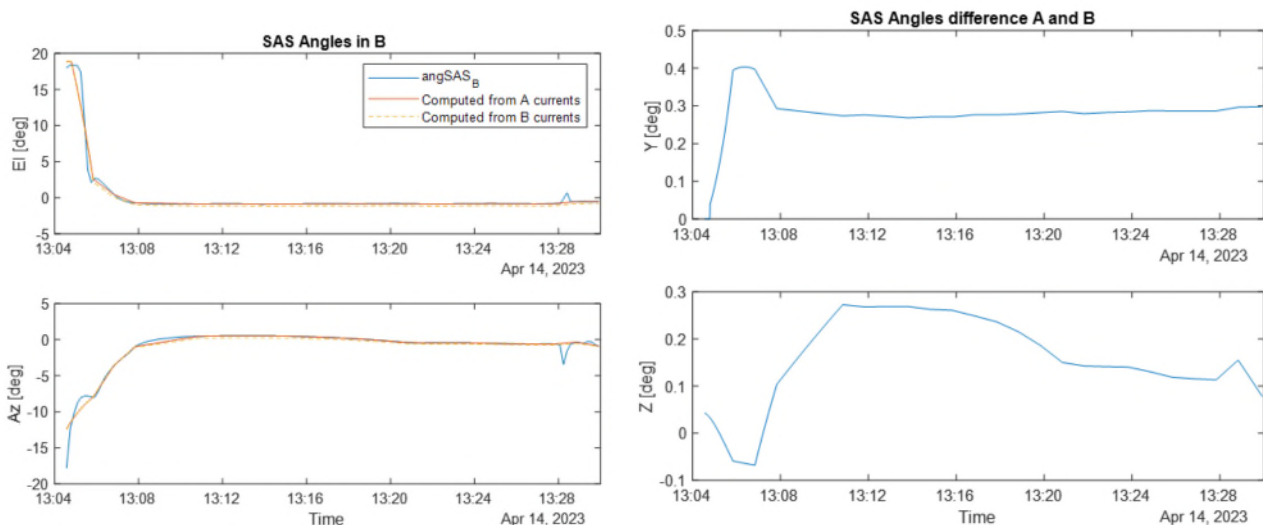

Figure 12. SAS angles computed from raw current acquisitions (left) and difference between prime and redundant (right)

In addition, as a sanity check, the expected SAS readings were computed using the predicted ideal trajectory obtained from SPICE and the STR readings. The measurement trend was observed to be the same, providing confidence on the sensor readings. Note that the observed bias is within the expected SAS alignment, but cannot be solely attributed to alignment due to the use of inaccurate orbit information.
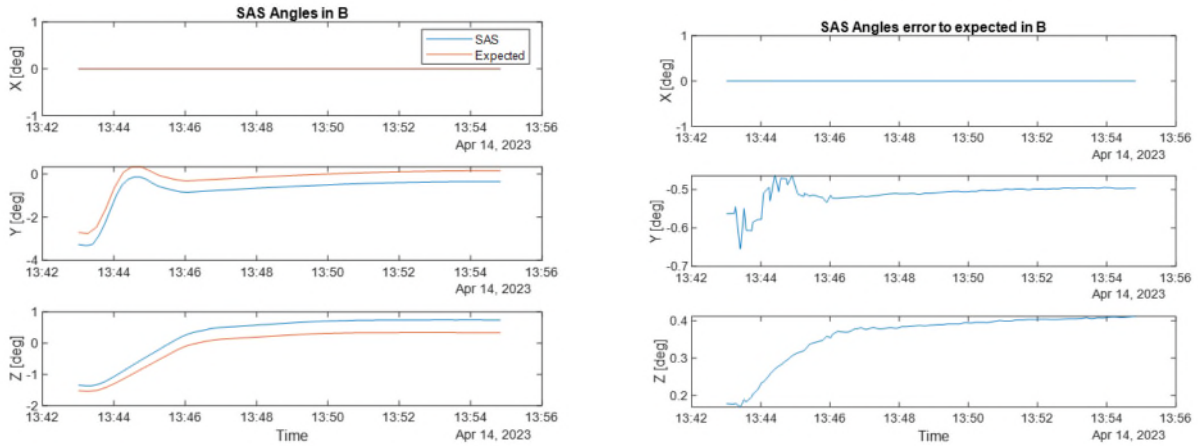

Figure 13. SAS Angle readings vs expected sun position from predicted orbit and STR attitude

Body Rates

IMU readings (angRateMeas_B) were compared to the on-board Gyro-Stellar Estimator (GSE) estimate as well as to the rates computed using the STR quaternion to check the correct working of the GSE. These are shown on the left side of the figure below. In addition, the rates during a dynamic period were computed using the thruster actuations by integrating the attitude dynamics. This provides a qualitative measure to increase confidence in the system. The results are shown on the right side of the figure below.
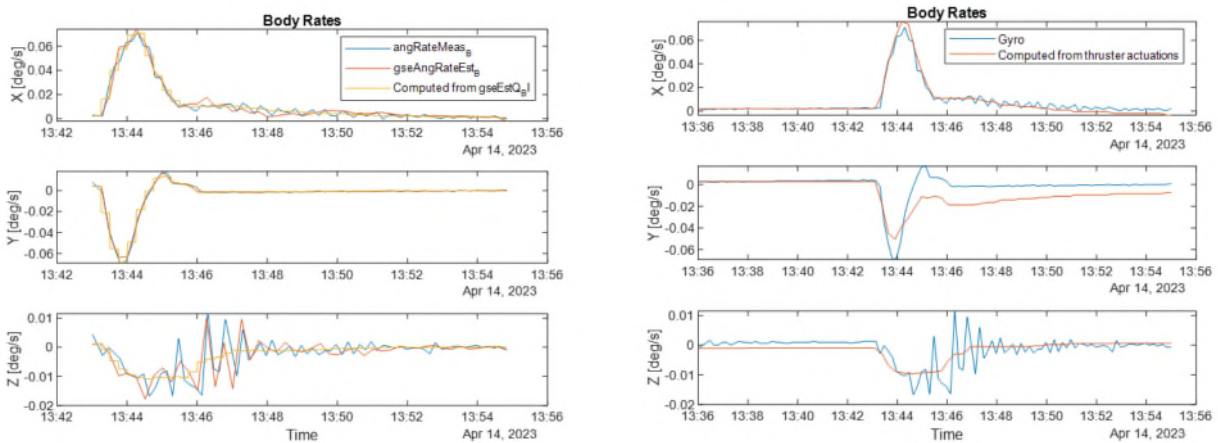

Figure 14. Body rate consistency between IMU/STR (left) and IMU/Thruster Actuations (right)

Star Trackers

The star trackers were switched on by the automatic separation sequence at 13:43, and were observed to be tracking no less than 13 stars on each Optical Head (OH) which was considered very good. This was later re-checked for a longer period in order to determine the quality of the tracking. For this purpose, the number of lost stars (right side of the figure below) for each head was computed using the number of tracked stars (left side of the figure below) and the expected number of stars in the FoV of each head.
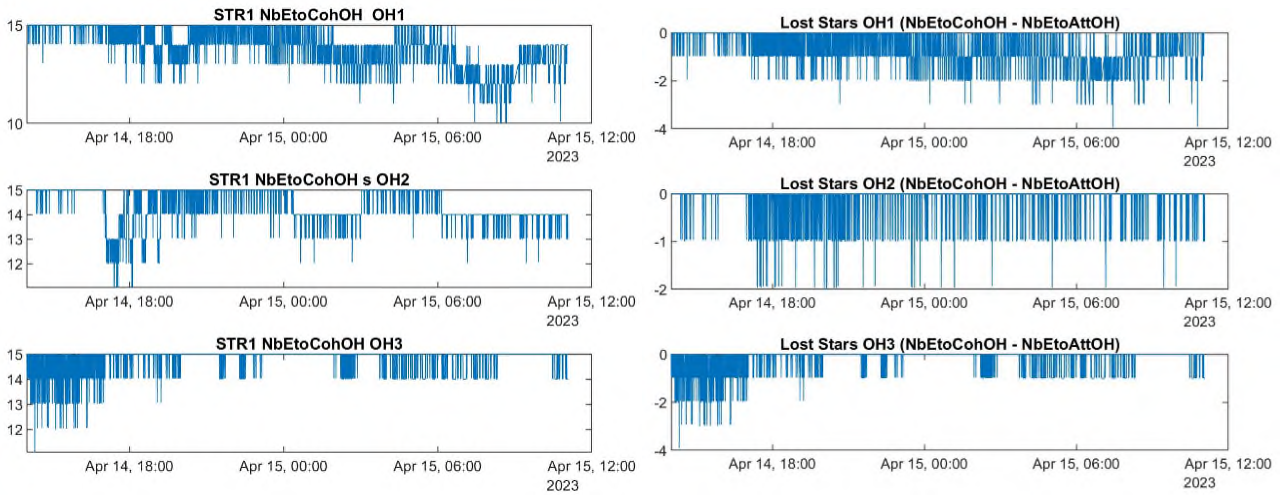
Figure 15. STR Number of tracked stars (left) and lost stars (right)

In addition, the inter-head misalignments were initially observed to be less than 60 arcsec, but were observed to grow to around 100 arcsec as the trackers cooled over the next few hours. Part of this initial misalignment was also attributed to the fact that the relativistic correction was not implemented yet as the velocity was set to zero. However, given the initial spacecraft velocity with respect to the solar system barycentre of around 30km/s, the worst-case effect was computed to contribute a possible maximum of 12arcsec to the misalignment. The observed angles, shown in the figure below, show that OH2 was misaligned more (~80as) with respect to the other 2 heads which exhibit a relative alignment of about ~20as. As it is impossible to tell which one is really correct, it was later decided to calibrate the OH alignment with respect to the average solution of the three heads.
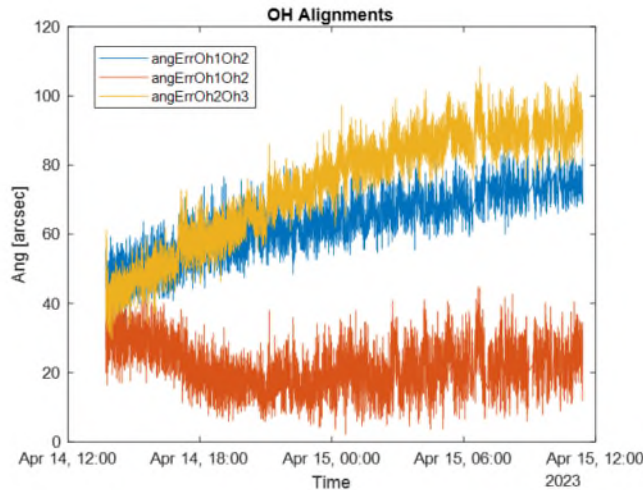

Figure 16. STR OH Alignments

Disturbance torques and fuel consumption in SAM SBP
The external disturbance torques were computed from thruster actuations and were observed to be slightly higher than the expected Solar Radiation Pressure (SRP). Further monitoring showed a progressive drop over the first two hours, consistent with outgassing. The figure below shows the accumulated torques from thruster actuations along with the slopes of a linear fit. The expected SRP level was around ~ 8e-5 Nm. The fuel consumption in this phase was estimated at ~3g/hour.
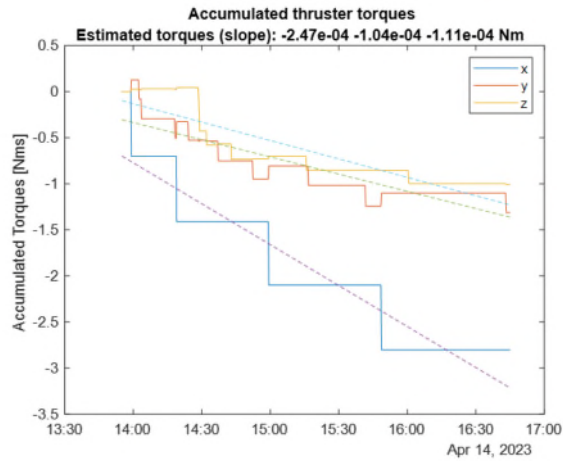
Figure 17. Estimated disturbance torque during SAM SBP in thruster control

3.4 Transition to Safe Hold Mode

Once the AOCS was established to be healthy, it was authorized to transition to "Safe Hold Mode" (SHM) / "Thruster Control Phase" (TCP), the first mode using the Gyro-Stellar Estimator and thrusters for control.

3.5 Reaction Wheel Activation

The reaction wheels were first activated in speed mode outside of the control loop, in order to run them in after the launch and establish their health before being used for control. Each of the 4 RWs were switched on sequentially and spun to a low momentum setpoint of +/-20Nms. The friction torques all stabilized below the nominal values after only 15 minutes. This was extremely fast with respect to the expected 6h to 24h stated in the user manual as the required run-in time for the friction torque to drop below the 25mNm threshold at nominal speeds. The figure below shows the initial friction torque peak after first activation and stabilization over the next 12h along with the bearing temperature and motor power. Note that the oscillations observed around 21:00 correspond to the transition to wheel-based control when the wheels present some slight transients in their momentum as they absorb the body residual rates from the thruster based control. The oscillations present in the friction torque after a few hours in wheels 3 and 4 are considered nominal oil redistribution effects.
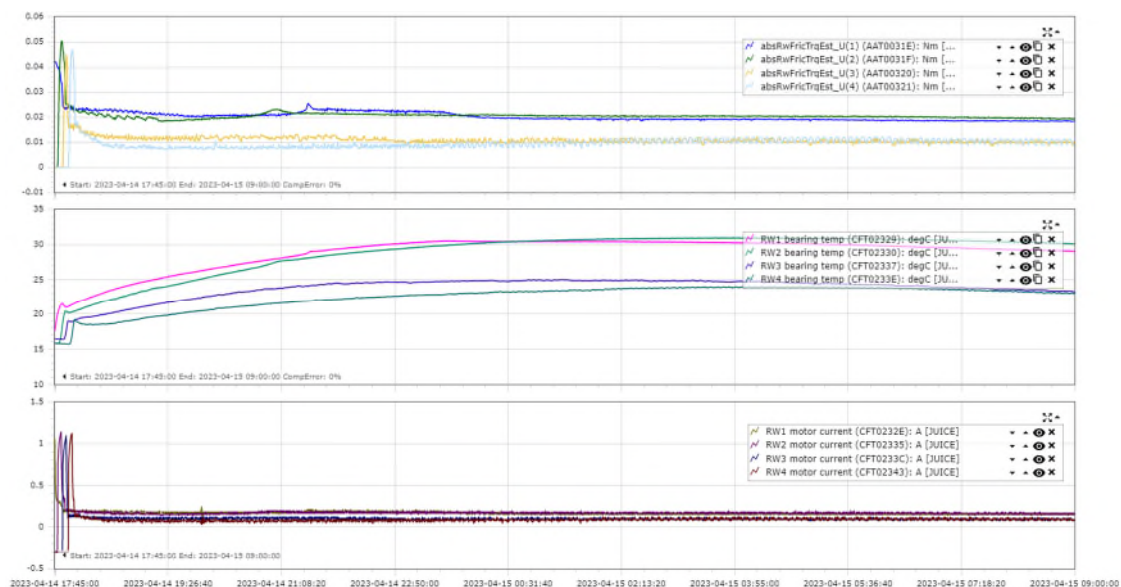

Figure 18. Reaction Wheel Friction Torque

3.6   Transition to Wheel Based mode

Transition to the first wheel based mode, SHM/Coarse Pointing Phase (CPP), was authorized very early due to the fast convergence of the reaction wheel friction torque. This was followed by transition to Normal Mode (NM). The figure below shows the control angular errors exhibiting the traditional two-sided limit cycle with thrusters becoming tighter at transition to wheel control.
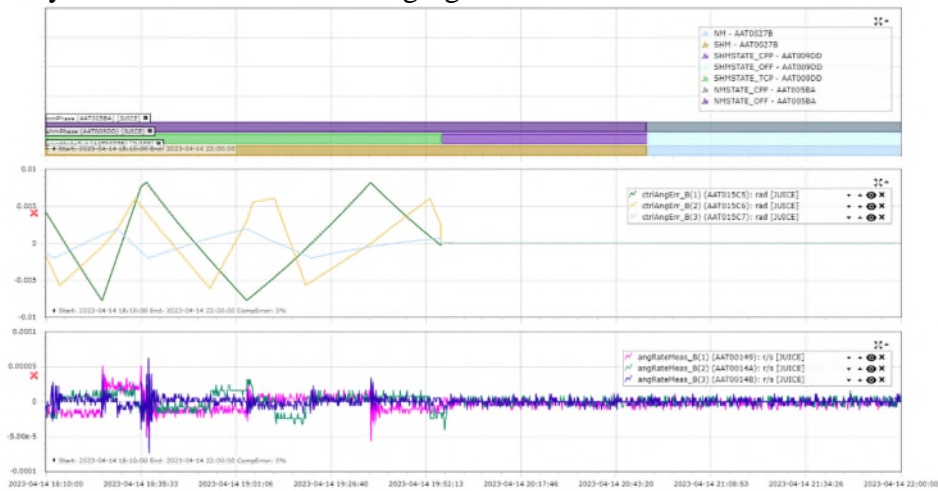

Figure 19. Transition to wheel control

3.7   Flexible Mode Characterization

To characterize the spacecraft flexible modes in support to thruster PWM frequency retuning and Main Engine Shaping pulse retuning, a series of thruster pulses were generated to produce torques on each of the body axis. Using the spacecraft body rates with high frequency telemetry at 8Hz, the flexible response of the appendages can be computed. The pulses were generated using the wheel offloading function of the spacecraft in order to simplify the attitude control during the operations. A wheel offloading target is computed to yield a single pure pulse on each axis. This operation was performed before and after Magboom deployment, and with different solar array orientations to allow decoupling of the different modes. The figure below shows the spacecraft rate on the X axis for one of these pulse after Magboom deployment. The secondary modes are visible on the zoom of the temporal plots.
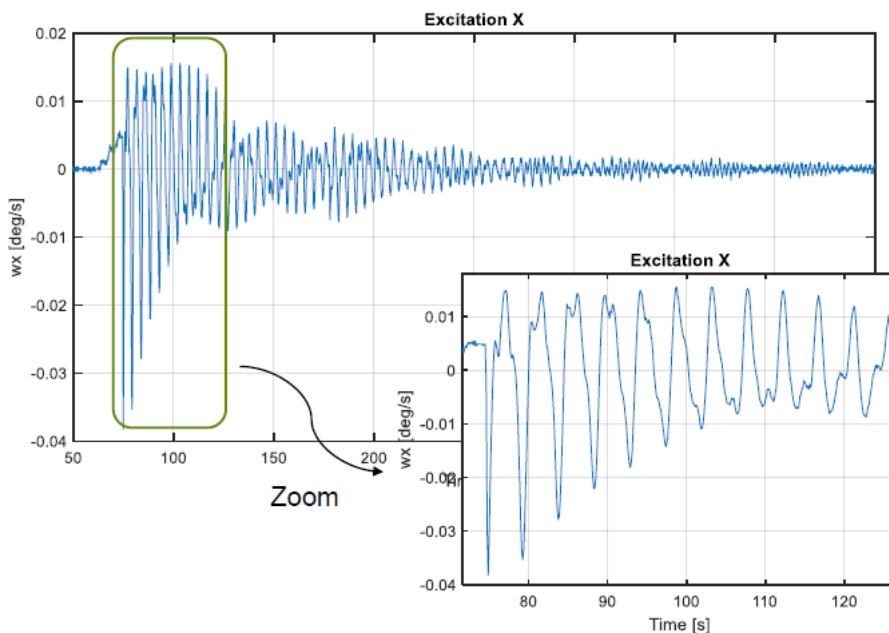

Figure 20. Flexible mode characterization, spacecraft response to thruster pulse

The final figure shows the FFT results of the body rate signals, showing the correlation of the flexible modes to their expected locations from the flexible models.
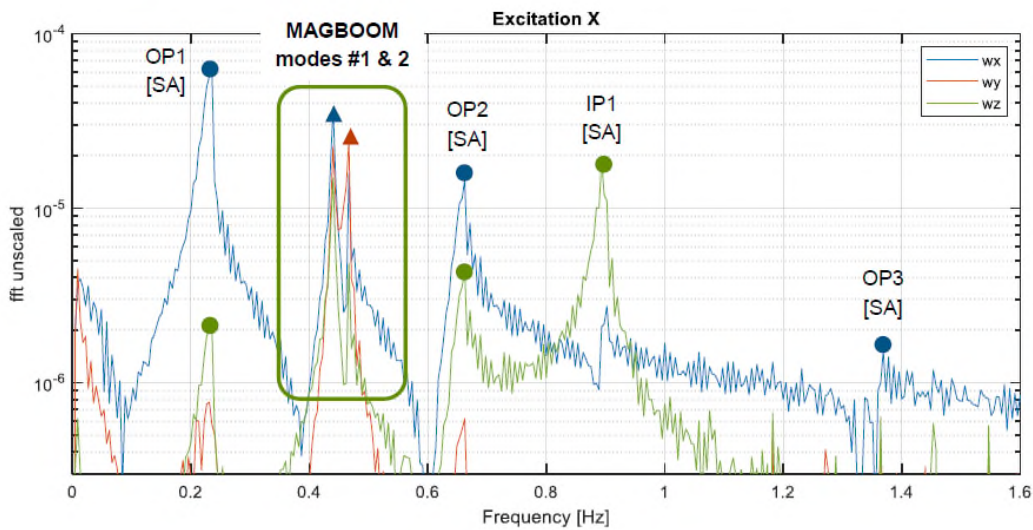

Figure 21. Flexible mode characterization, after FFT pos-processing

3.8   Trajectory Manoeuvre Modes

The two trajectory manoeuvre modes, namely the Orbit Control Mode using four 22N thrusters, and the Main Engine Boost Mode using a thrust ramp-up from the 22N thruster followed by a Main Engine burn phase encompassing shaping pulses were also tested successfully, showing excellent performance.

The introduction of main engine shaping pulses is an AOCS innovation aimed at minimizing the oscillations of the solar arrays Out-Of-Plane mass flexible mode under large S/C accelerations (see reference 3), which proved very efficient when comparing accelerometer measurements after MEBM with ones acquired during open-loop Main Engine pulses performed to help deploying RIME.
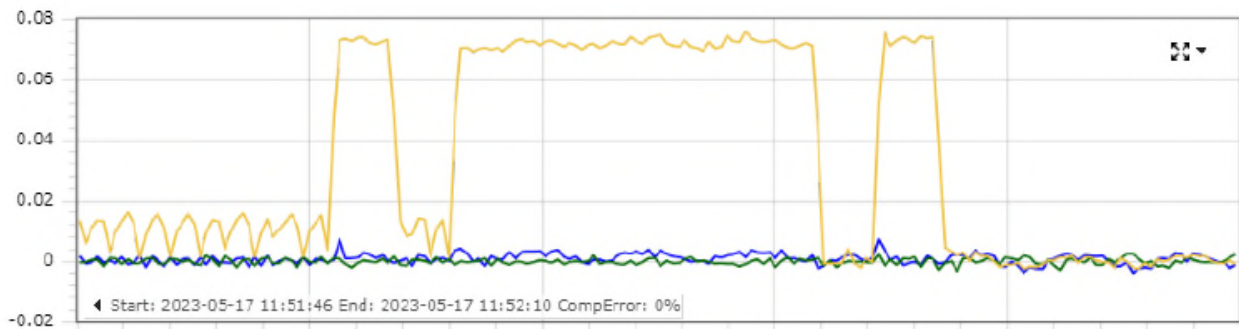

Figure 22. MEBM acceleration profile as measured by accelerometers (vertical bars every 5s)

4   REFERENCES

[1] Benoît Gelin, Guillaume Montay, Yannick Henriquel, Jean-Frédérick Bouvry, Pascal Regnier and Daniele Gherardi, *Hydra Star Tracker for Juice Mission (AAS 18-104)*

[2] Gorog F., *JUICE Navigation Camera Design"*, SODERN, ESA GNC Conference 2021

[3] Regnier P, Guignard A., Gherardi D., *JUICE AOCS : an optimal combination of Airbus DS interplanetary AOCS heritage and efficient GNC innovations,* ESA GNC Conference 2017